Laminar Liquid Jet Diffusion Studies

J. L. DUDA and J. S. VRENTAS

The Dow Chemical Company, Midland, Michigan

A rigorous analysis of jet hydrodynamics is used to develop a technique for determining diffusion coefficients from laminar liquid jet absorption experiments, and the influence of the jet fluid mechanics on the absorption process is clarified. The new technique is used to determine the diffusivities of carbon dioxide, oxygen, argon, nitrous oxide, ethylene, and propylene in water within the temperature range 25° to 40°C.

A critical analysis of available diffusivity data for these gases indicates that there is no conclusive evidence that demonstrates the existence of a significant interfacial resistance in uncontaminated laminar jet experiments. In addition, comparison of existing data shows that the commonly accepted diffusivities for the oxygen-water system may be significantly higher than the actual values. It is concluded that the laminar jet experiment is a rapid, accurate method of obtaining diffusion coefficients of dissolved gases in liquids.

In order to determine the diffusion coefficients of dissolved gases in liquids, various experimental techniques have been devised (*15*). Of these, laminar liquid jets possess several distinct advantages over other methods and consequently have been employed in numerous studies (*6, 7, 38*). However, there are still two uncertainties associated with jet absorption studies which must be resolved before this experimental technique can gain wide acceptance as an accurate method of measuring diffusion coefficients.

The first uncertainty associated with this technique, as well as with other methods involving mass transfer across gas-liquid interfaces, is the possible existence of a significant resistance to mass transfer at the phase interface. In order to obtain diffusivities from jet absorption data it must be assumed that the interface is at all times saturated with the gas being absorbed. In reality, the gas molecules are transferred to the liquid interface at a finite rate, thus creating an extra resistance to mass transfer. This resistance will be particularly apparent during the short contact times realized with a laminar jet when the liquid-phase resistance is still relatively small. There are some indications, particularly the studies of Chiang and Toor (*6*) and Baird and Davidson (*2*), that this interfacial resistance is large enough to make the rate of gas absorption into laminar jets of pure liquids significantly different from that predicted with the assumption that there is equilibrium at the interface. If this is indeed the case, short contact time equipment like laminar jets can be of little use in the measurement of diffusivities of dissolved gases in liquids.

The second uncertainty is the influence of the jet hydrodynamics on the rate of mass transfer. Since both an interfacial resistance and a hydrodynamic effect tend to reduce the mass transfer that would be realized in an idealized jet, the effects of these two phenomena are difficult to isolate. Although the fluid mechanics of laminar jets is more tractable than other flow configurations, the exact influence of the flow field on the mass transport process has never been completely determined. Scriven and Pigford (*31*) presented an approximate analysis to the problem of describing mass and momentum transport in laminar liquid jets. However, instead of theoretically incorporating the influence of the jet hydrodynamics in the analysis of the absorption data, most investigators have attempted to reduce these effects experimentally (*7, 28*) by employing special nozzles which inhibit the development of a velocity profile in the nozzle region. Owing to the flow adjacent to fixed walls, however, the surface of the jet must always leave a nozzle with a velocity approaching zero. Therefore, it is impossible to design a nozzle that will produce a perfectly flat initial velocity profile, and the influence of the hydrodynamics during the relaxation of the initial profile can be completely resolved

only by a theoretical analysis.

In this study a recent rigorous analysis of jet hydrodynamics (*10*) is employed in the development of a technique for the analysis of jet absorption data; the uncertainty associated with the relaxation of the initial velocity profile is thus effectively eliminated. The developed method of analysis is then used to obtain diffusivity data from the jet absorption data of six gases in water. These results are then compared with diffusivity values available in the literature, and an attempt is made to determine the accuracy of the jet technique and to resolve the question of the existence of a significant interfacial resistance.

EXPERIMENT

The laminar liquid jet apparatus used in this study was similar to that described elsewhere (*42*). The major components of this apparatus are a thermostatic absorption chamber, a constant head water feed system, and a constant pressure gas feed system with a soap-film meter.

In the water feed system, deionized water was stripped of dissolved gases, cooled to the absorption temperature, and metered to the absorption chamber. This water stream was analyzed by a polarographic method for oxygen concentration so that a correction for the desorption of dissolved nitrogen and oxygen could be included in the analysis of the absorption data. This correction was in all cases less than 3%. The laminar jet was formed by a stainless steel nozzle consisting of an elliptic shaped converging section followed by a 0.9 mm. cyindrical throat with an inside diameter of 0.1591 cm. The throat and face of the nozzle were polished to a smooth finish, and the face was coated with a thin film of paraffin wax to prevent wetting. The nozzle was mounted on the end of a stainless steel tube which had a horizontal traversing mechanism that permitted adjustment over the jet receiver and a vertical adjustment which controlled the jet length which was measured with a cathetometer. The jet flow rate was varied from 300 to 470 g./min., and the jet length was varied from 1 to 10 cm. The very short cylindrical throat of the nozzle made it possible to produce laminar jets at relatively high Reynolds numbers. A pyrex jet receiver was constructed from a 1 cm. length of capillary tubing of 2 mm. I.D. attached to a 5 cm. piece of 25 mm. tubing. The proper capillary seal at the mouth of the receiver was obtained by the use of a sensitive liquid level control valve.

Before entering the absorption chamber the gas was saturated with water at the absorption temperature and then passed through the soap-film meter. The rate of absorption was determined by timing the ascent of a soap bubble in a graduated glass tube. The absorption chamber and soap-film meter were enclosed in a constant temperature air box which could be controlled to ±0.01°C. In addition, the absorption chamber was equipped with a water jacket, so that it was estimated that the temperature within the chamber could be controlled to less than ±0.01°C.

THEORY

In order to deduce precise diffusion coefficients from a laminar liquid jet apparatus, it is necessary to formulate a relatively accurate analysis of the mass and momentum transport in the jet flow field. We consider the laminar flow behavior of a vertical jet of a Newtonian liquid issuing from a circular nozzle under steady state, isothermal flow conditions. It will further be assumed that there is symmetry in the azimuthal direction, the velocity in this direction is everywhere equal to zero, and the outer fluid is inviscid and at constant pressure. Finally, since the amount of the outer gas phase absorbed is very slight, the density and viscosity of the liquid jet will be considered constant, and any phase change due to mass transfer is neglected. Consequently, the equations of motion and the equation of species continuity are uncoupled, and the fluid mechanics and mass transfer can be considered separately.

Fluid Mechanics

Since the Reynolds numbers of the jets used in this investigation are relatively high, axial diffusion of vorticity can be neglected, and the velocity field in a jet can be calculated by analyzing the flow in the nozzle first and then by using the velocity profile at the exit of the nozzle as an initial condition for the solution of the equations of motion describing the jet itself. It is assumed that the velocity profile entering the cylindrical throat of the nozzle is uniform; thus, the velocity distribution at the exit of the cylindrical throat can be easily deduced by a finite-difference solution of the boundary-layer representation of the equations of motion (*41*). The velocity field in the jet can then be obtained by a finite-difference solution (*10*) of the following set of equations and boundary conditions written in dimensionless form:

$$\frac{\partial \phi}{\partial \zeta} = N_J + \frac{2}{N_{We}(R_s^2)^{3/2}} \frac{dR_s^2}{\partial \zeta} + 4\left[\frac{\partial \phi}{\partial \psi} + \frac{r^2\sqrt{\phi}}{2}\frac{\partial^2 \phi}{\partial \psi^2}\right] \tag{1}$$

$$\phi = U^2 \tag{2}$$

$$N_J = \frac{N_{Re}}{N_{Fr}} \tag{3}$$

$$\frac{\partial r^2}{\partial \psi} = \frac{2}{\sqrt{\phi}} \tag{4}$$

$$VN_{Re} = U\frac{\partial r}{\partial \zeta} \tag{5}$$

$$\frac{\partial \phi}{\partial \psi} = \frac{1}{4}\left[\frac{\partial \phi}{\partial \zeta} - N_J - \frac{2}{N_{We}(R_s^2)^{3/2}}\frac{dR_s^2}{d\zeta}\right] \quad \text{for } \psi = 0,\ \zeta > 0 \tag{6}$$

$$\phi(\psi, 0) = g(\psi) \tag{7}$$

$$\frac{\partial \phi}{\partial \psi} = 0 \text{ for } \psi = \tfrac{1}{2},\ \zeta > 0 \tag{8}$$

$$r^2(0, \zeta) = 0 \tag{9}$$

The function $g(\psi)$ is, of course, deduced from the analysis of the flow field in the cylindrical throat of the nozzle. The solution of the above equations of change for the jet produces the following results which are to be used in the analysis of the mass transfer:

$$U = F[\zeta, \psi, N_J, N_{We}, g(\psi)] \tag{10}$$

$$VN_{Re} = G[\zeta, \psi, N_J, N_{We}, g(\psi)] \tag{11}$$

$$r^2 = H[\zeta, \psi, N_J, N_{We}, g(\psi)] \tag{12}$$

Mass Transfer

In the analysis of the gas absorption into the liquid jet it is helpful to utilize the concept of Protean coordinates (*10*) in much the same fashion as in the determination of the velocity field. In general, the species continuity equation at steady state can be written as

$$(\rho_I v^i)_{,i} + (j_I{}^i)_{,i} = 0 \tag{13}$$

with the diffusion flux given by

$$j_I{}^i = -g^{ij}\,\rho D\frac{\partial \omega_I}{\partial X^j} \tag{14}$$

Since the diffusion coefficient can be considered constant and the liquid phase incompressible, Equations (13) and (14) can be combined to give the following equation in Protean coordinates:

$$\overline{v}^i\frac{\partial \rho_I}{\partial \overline{X}^i} - \frac{D}{\overline{g}^{1/2}}\frac{\partial}{\partial \overline{X}^i}\left(\overline{g}^{1/2}\,\overline{g}^{ij}\frac{\partial \rho_I}{\partial \overline{X}^j}\right) = 0 \tag{15}$$

The Protean coordinates are chosen as

$$\overline{X}^1 = \psi \quad \overline{X}^2 = \theta \quad \overline{X}^3 = \xi \tag{16}$$

and useful relationships to cylindrical coordinates are given by (*10*)

$$\overline{v}^1 = 0 \quad \overline{v}^2 = 0 \quad \overline{v}^3 = v^3 \tag{17}$$

$$[\overline{g}^{ij}] = \begin{bmatrix} r^2[(v^3)^2 + (v^1)^2] & 0 & -rv^1 \\ 0 & \dfrac{1}{r^2} & 0 \\ -rv^1 & 0 & 1 \end{bmatrix} \tag{18}$$

$$\overline{g} = \frac{1}{(v^3)^2} \tag{19}$$

Consequently, from Equations (16) to (19) it follows that the dimensionless form of Equation (15) can be written as

$$U\frac{\partial \rho_I}{\partial \xi} + \frac{2}{N_{Re}N_{Sc}}\left[-r^2(U^2+V^2)\frac{\partial^2 \rho_I}{\partial \psi^2} + 2rV\frac{\partial^2 \rho_I}{\partial \xi \partial \psi} - \frac{\partial^2 \rho_I}{\partial \xi^2} - 2U\frac{\partial \rho_I}{\partial \psi} + r\frac{\partial V}{\partial \xi}\frac{\partial \rho_I}{\partial \psi} - r^2U\frac{\partial U}{\partial \psi}\frac{\partial \rho_I}{\partial \psi} - r^2V\frac{\partial \rho_I}{\partial \psi}\frac{\partial V}{\partial \psi}\right] = 0 \tag{20}$$

Under ordinary experimental conditions, axial diffusion of the dissolved gas in liquid jets is negligible, and Equation (20) can be reduced to

$$\frac{\partial \rho_I}{\partial \zeta} = \frac{2}{N_{Sc}}\left[r^2U\frac{\partial^2 \rho_I}{\partial \psi^2} + r^2\frac{\partial U}{\partial \psi}\frac{\partial \rho_I}{\partial \psi} + 2\frac{\partial \rho_I}{\partial \psi}\right] \tag{21}$$

with boundary conditions

$$\rho_I(\psi, 0) = 0 \tag{22}$$

$$\rho_I\left(\frac{1}{2}, \zeta\right) = 1 \tag{23}$$

$$\left(\frac{\partial \rho_I}{\partial \psi}\right)_{\psi=0} = \frac{N_{Sc}}{4}\left(\frac{\partial \rho_I}{\partial \zeta}\right)_{\psi=0} \tag{24}$$

The inlet concentration is assumed to be uniform, and the jet surface at $\psi = \frac{1}{2}$ is assumed to be at equilibrium with the essentially pure gas phase.

Equations (21) to (24) can be solved for the concentration field for a given value of D by standard finite-difference considerations. However, since the purpose of this investigation is to extract D from the absorption data, it is more convenient to derive an analytical expression involving the diffusion coefficient rather than to substitute different values of D into Equations (21) to (24), solve the equations numerically, and choose the value whose calculated absorption rate most closely agrees with the experimental data. Hence, we capitalize on the high Schmidt number and relatively small penetration depth characteristic of the usual jet experiment to obtain a perturbation solution of Equation (21). If we let

$$Y = \frac{1}{2} - \psi \tag{25}$$

we can write Taylor series expansions for U, r^2, and $\partial U/\partial Y$ as follows:

$$U(\zeta, Y) = U(\zeta, 0) + \left(\frac{\partial U}{\partial Y}\right)_{Y=0} Y + \dots \tag{26}$$

$$r^2(\zeta, Y) = r^2(\zeta, 0) + \left(\frac{\partial r^2}{\partial Y}\right)_{Y=0} Y + \dots \tag{27}$$

$$\frac{\partial U}{\partial Y}(\zeta, Y) = \frac{\partial U}{\partial Y}(\zeta, 0) + \left[\frac{\partial}{\partial Y}\left(\frac{\partial U}{\partial Y}\right)\right]_{Y=0} Y + \dots \tag{28}$$

In addition, introduction of the variable

$$\eta = Y\, N_{Sc}^{1/2} \tag{29}$$

converts Equations (21) to (24) to

$$\frac{\partial \rho_I}{\partial \zeta} = 2\, r^2\, U\frac{\partial^2 \rho_I}{\partial \eta^2} + \frac{2\, r^2}{\sqrt{N_{Sc}}}\frac{\partial \rho_I}{\partial \eta}\frac{\partial U}{\partial Y} - \frac{4}{\sqrt{N_{Sc}}}\frac{\partial \rho_I}{\partial \eta} \tag{30}$$

$$\rho_I(\eta, 0) = 0 \tag{31}$$

$$\rho_I(0, \zeta) = 1 \tag{32}$$

$$\rho_I(\infty, \zeta) = 0 \tag{33}$$

Utilization of Equation (33) is permissible if the contact times of the jet experiment are such that the center of the jet is negligibly influenced by the absorption at the jet surface.

A perturbation solution of Equations (30) to (33) can now be effected by introducing a series expansion in terms of ascending powers of the small parameter $N_{Sc}^{-1/2}$:

$$\rho_I(\eta, \zeta) = \rho_I^0(\eta, \zeta) + N_{Sc}^{-1/2}\rho_I^1(\eta, \zeta) + (N_{Sc}^{-1/2})^2\rho_I^2(\eta, \zeta) + \dots \tag{34}$$

Substitution of Equations (26) to (29) and Equation (34) into Equations (30) to (33), utilization of Equations (4) and (8), and introduction of the condition that the coefficients of each power of $N_{Sc}^{-1/2}$ must separately vanish give the following equations for the zero-order and first-order terms of the perturbation series:

$$\frac{\partial \rho_I^0}{\partial \zeta} = 2\, U_s R_s^2 \frac{\partial^2 \rho_I^0}{\partial \eta^2} \tag{35}$$

$$\rho_I^0(\eta, 0) = 0 \tag{36}$$

$$\rho_I^0(0, \zeta) = 1 \tag{37}$$

$$\rho_I^0(\infty, \zeta) = 0 \tag{38}$$

$$\frac{\partial \rho_I^1}{\partial \zeta} = 2U_sR_s^2\frac{\partial^2 \rho_I^1}{\partial \eta^2} - 4\eta\frac{\partial^2 \rho_I^0}{\partial \eta^2} - 4\frac{\partial \rho_I^0}{\partial \eta} \tag{39}$$

$$\rho_I^1(\eta, 0) = \rho_I^1(0, \zeta) = \rho_I^1(\infty, \zeta) = 0 \tag{40}$$

The solution to Equations (35) to (38) is simply (*5*)

$$\rho_I^0 = \operatorname{erfc}\left(\frac{\eta\sqrt{2}}{4\sqrt{\tau}}\right) \tag{41}$$

where

$$\tau = \int_0^\zeta R_s^2\, U_s\, d\zeta \tag{42}$$

From Equation (41) it follows that Equation (39) becomes

$$\frac{\partial \rho_I^1}{\partial \zeta} = 2\, U_sR_s^2\frac{\partial^2 \rho_I^1}{\partial \eta^2} - \frac{1}{2}\sqrt{\frac{2}{\pi}}\frac{\eta^2}{\tau^{3/2}}e^{-\eta^2/8\tau} + 2\sqrt{\frac{2}{\pi\tau}}e^{-\eta^2/8\tau} \tag{43}$$

Utilization of a transformation of variables from ζ to τ and application of Duhamel's theorem (5) give the following solution to Equation (43) and its homogeneous boundary conditions:

$$\rho_I{}^1 = \int_o^\tau \frac{1}{R_s{}^2\, U_s}\left[-\frac{2\eta\,\lambda^{1/2}\, e^{-\eta^2/8(\tau-\lambda)}}{\pi(\tau-\lambda)^{3/2}} + \frac{2\lambda}{\tau^{3/2}}\sqrt{\frac{2}{\pi}}\, e^{-\eta^2/8\tau}\,\mathrm{erf}\left(\eta\sqrt{\frac{\lambda}{8\tau(\tau-\lambda)}}\right) - \frac{\lambda\eta^2}{2\tau^{5/2}}\sqrt{\frac{2}{\pi}}\, e^{-\eta^2/8\tau}\,\mathrm{erf}\left(\eta\sqrt{\frac{\lambda}{8\tau(\tau-\lambda)}}\right) + \frac{2\lambda^{3/2}\eta}{\pi\tau^2}\,\frac{(2\tau-\lambda)}{(\tau-\lambda)^{3/2}}\, e^{-\eta^2/8(\tau-\lambda)}\right] d\lambda \qquad (44)$$

Table 1 indicates how well the first two terms of the perturbation series as represented by Equations (34), (41), and (44) approximate a finite-difference solution to Equations (21) to (24) for a jet with hydrodynamics and Schmidt number characteristic of a typical jet diffusion experiment. The mass densities shown in the table were evaluated for different jet lengths at $\psi = 0.45$. It is clear that the zero-order perturbation solution alone is insufficient for accurate determination at these points. Closer to the jet surface, the zero-order solution provides a better approximation to the finite-difference solution. Second-order and higher-order perturbation terms were not evaluated. It is evident that the inclusion of such terms would require a more detailed knowledge of the velocity field and the curvature of the streamlines.

Table 1. Comparison of Numerical and Perturbation Solutions of Diffusion in Laminar Jets

ρ_I, finite-difference solution	ρ_I, zero-order perturbation solution	ρ_I, zero-order and first-order perturbation solution
0.0628	0.0695	0.0624
0.155	0.166	0.156
0.189	0.200	0.190

In the jet experiment the quantity measured directly is the mass of gas absorbed per unit time. This quantity is related to the absorption rate per unit area N_I by the equation

$$Q = \int_o^\xi 2\pi\, R_s(\xi)\, N_I(\xi)\, R_o{}^2\sqrt{1+\left(\frac{V_s}{U_s}\right)^2}\, d\xi \qquad (45)$$

which is derived by considering the geometrical character of the gas-liquid interface. The mass of gas absorbed into the jet per unit time per unit area is given by the scalar product of the diffusion flux at the surface and the unit normal vector to the surface pointing into the liquid phase:

$$N_I = \bar{j}_I{}^i\, \bar{n}_i = -\bar{n}^j\, D\frac{\partial \rho_I}{\partial \bar{X}^j} \qquad (46)$$

From the contravariant components of the unit normal vector to the phase interface (10)

$$\bar{n}^1 = -r\sqrt{(v3)^2+(v1)^2} \qquad (47)$$

$$\bar{n}^2 = 0 \qquad (48)$$

$$\bar{n}^3 = \frac{v^1}{\sqrt{(v3)^2+(v1)^2}} \qquad (49)$$

it follows that Equation (46) can be expressed as

$$\frac{N_I\, R_o}{D(\rho_{IE}-\rho_{IO})} = R_s\,(U_s{}^2+V_s{}^2)^{1/2}\left(\frac{\partial \rho_I}{\partial \psi}\right)_{\psi=1/2} \qquad (50)$$

where from Equations (34), (41), and (44) it is evident that

$$\left(\frac{\partial \rho_I}{\partial \psi}\right)_{\psi=1/2} = \sqrt{\frac{N_{Sc}}{2\pi\tau}} - \int_o^\tau \frac{2\lambda^{3/2}}{R_s{}^2\, U_s\, \pi\tau^2(\tau-\lambda)^{1/2}}\, d\lambda \qquad (51)$$

Consequently, Equation (45) becomes

$$\frac{Q}{2\pi\, D(\rho_{IE}-\rho_{IO})\, R_o} = \int_o^\xi R_s{}^2\, U_s\left(\frac{\partial \rho_I}{\partial \psi}\right)_{\psi=1/2} d\xi + \int_o^\xi \frac{R_s{}^2\, V_s{}^2}{U_s}\left(\frac{\partial \rho_I}{\partial \psi}\right)_{\psi=1/2} d\xi \qquad (52)$$

Equations (51) and (52) can be used in conjunction with Equations (10), (11), (12), and (42) to derive diffusion coefficients from Q vs. jet length data. However, there are two simplifications which can be used to reduce these equations further. First of all, for the usual jet experiment and certainly for this investigation, the second integral in Equation (52) is completely negligible. Furthermore, for the small contact times used here, calculations show that the second term of Equation (51) is a small fraction of the first term. Equation (51) serves as a convenient check to guarantee that the zero-order perturbation is sufficient to accurately describe the jet absorption rate. Hence, from Equations (51) and (52) it follows that

$$\Omega = \frac{Q}{4\,\pi^{1/2}\, R_o{}^{3/2}\, U_a{}^{1/2}\, N_{Re}{}^{1/2}\,(\rho_{IE}-\rho_{IO})} = D^{1/2}\,\tau^{1/2} \qquad (53)$$

which is the equation used in this study to obtain diffusion coefficients.

If it can be assumed that the velocity profile of the jet is uniform at every jet length, it is evident that

$$R_s{}^2\, U_s = 1 \qquad (54)$$

$$\tau = \zeta \qquad (55)$$

and Equation (53) reduces to

$$\frac{Q}{4\,\pi^{1/2}\, R_o{}^{3/2}\, U_a{}^{1/2}\,(\rho_{IE}-\rho_{IO})} = D^{1/2}\,\xi^{1/2} \qquad (56)$$

Equation (56) is equivalent to that derived by considering diffusion in the rodlike flow of a semi-infinite sheet of liquid and by applying the results to a cylindrical jet of constant diameter. Hence, as previously noted by Cullen and Davidson (8), the taper of the jet need not be considered if the velocity profile is essentially uniform at every jet length. Such an ideal situation can be approached by keeping the boundary layer in the jet as small as possible and by choosing jet lengths which are long enough so that the velocity profile relaxes essentially completely in a small fraction of the total jet length.

RESULTS AND DISCUSSION

Influence of Jet Fluid Mechanics

In order to establish the influence of the jet fluid mechanics on the absorption process, several jet flows in addition to the jets directly employed in this investigation were analyzed. In Figure 1 some of the results of these calculations are shown for a specific jet that was employed by Scriven and Pigford (*31*). This figure shows the behavior of both the dimensionless jet radius and the ratio of surface velocity to center-line velocity as functions of jet length. The excellent agreement between the calculated dependence of the radius and the experimentally measured points demonstrates the accuracy of the fluid mechanics analysis upon which the developments in this study are based. The flow behavior of the jets used in this investigation is similar to that of the jets employed by Scriven and Pigford. The slow approach to the value of one of the aforementioned velocity ratio indicates that the relaxation of the velocity profile can influence the absorption rate for significant jet lengths. Calculations were also performed for a jet similar in hydrodynamics to those employed by Chiang and Toor (*6*). In an attempt to inhibit the development of a velocity profile in the jet nozzle, Chiang and Toor used a thin orifice plate as a nozzle. However, the analysis of their jets shows that a more developed velocity profile at the nozzle exit was realized with the thin orifice than with the nozzles used in this investigation and the studies of Scriven and Pigford. This enhanced profile development is due to the fact that Chiang and Toor ran their jets at significantly lower Reynolds numbers. Conversely, the velocity profile in low Reynolds number jets relaxes over a shorter jet length than does the profile in high Reynolds number jets. In all the cases analyzed, essentially complete relaxation of the velocity profile was determined to take place farther down the jet than previous approximations of the jet hydrodynamics had indicated.

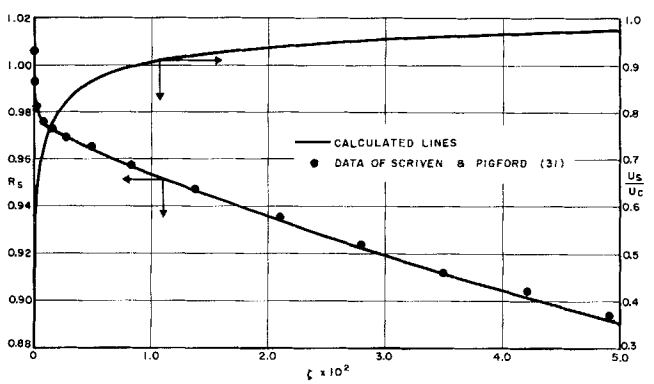

Fig. 1. Typical results of jet fluid mechanics calculations and comparison with experimental measurements of jet radius.

Equation (56) represents the commonly used method of analyzing jet absorption data based on the idealization that the velocity profile is flat over the entire length of the jet. A comparison of this idealized analysis with the technique developed in this study with Equation (53) demonstrates the error that is introduced into the calculated diffusion coefficient if the jet fluid mechanics is not included in the analysis. This comparison shows that for the jet hydrodynamics and lengths used in this investigation, a 10 to 15% error can be induced in the calculated diffusion coefficients. This error is reduced to a few percent for the jets employed by Chiang and Toor (even though calculations show that the jets contract to less than 75% of their nozzle radius), since the velocity profile relaxes in a small fraction of the longest jet length used by these investigators.

Diffusivity Results

For each of the six gases studied, absorption rate data were obtained at three flow rates and jet lengths varying from 1 to 10 cm. As a result, for each gas at a given temperature, from ten to twenty independent data points were obtained. Each of these points represents the average of at least twelve independent soap-film meter measurements. The small variation in ambient pressure was removed by correcting all absorption rates to a total pressure of 760 mm. The value of τ for each jet length was determined by a numerical integration of Equation (42) with values of jet radius and surface velocity obtained from a numerical solution of Equations (1) to (9) for the specific jet hydrodynamics used in the absorption experiments. The diffusion coefficients were determined from Equation (53) by plotting the group of variables on the left-hand side of this equation (this group includes the measured absorption rate) as a function of $\tau^{1/2}$ and evaluating the slope ($D^{1/2}$) of the best straight line with zero intercept by a least squares statistical analysis. The diffusivity results and the associated solubility data for all the cases studied are given in Table 2.

TABLE 2. EXPERIMENTAL DIFFUSION COEFFICIENTS OF DISSOLVED GASES IN WATER

Gas	Temp., °C.	Solubility × 10^5, g. mole/cc.	$D \times 10^5$, sq. cm./sec.	Reference for solubility
Oxygen	25	0.1224	2.07	32
Argon	25	0.1345	2.00	25
Carbon dioxide	25	3.303	1.98	25
Carbon dioxide	40	2.220	2.80	
Nitrous oxide	25	2.593	1.69	*23, 32*
Nitrous oxide	40	1.630	2.55	
Ethylene	25	0.4657	1.87	*33*
Ethylene	40	0.3500	2.53	
Propylene	25	0.6500	1.10	*1*
Propylene	40	0.3840	2.22	

Figures 2 and 3 show the best straight line and individual data points for argon at 25°C. and for carbon dioxide at 40°C. The scatter of the carbon dioxide data is typical of the majority of the cases studied. The scatter for the case of argon is greater owing to the low solubility of this gas and is also typical for the case of oxygen. The low solubilities of these two gases cause small absorption rates which are more difficult to measure accurately with the soap-film meter. The absorption rates can be increased by increasing the jet length, but absorption rates with longer jets showed a significant deviation from the correlation represented by Equation (53). This anomalous increase in absorption rate indicates that the jet may be approaching breakup and that the associated surface instabilities are significantly influencing the total absorption rate. Since these instabilities are not readily apparent from visual observation, deviation from the relationship presented by Equation (53) provides a method of determining the maximum allowable jet length for which the jet can be considered to exhibit well-defined laminar flow.

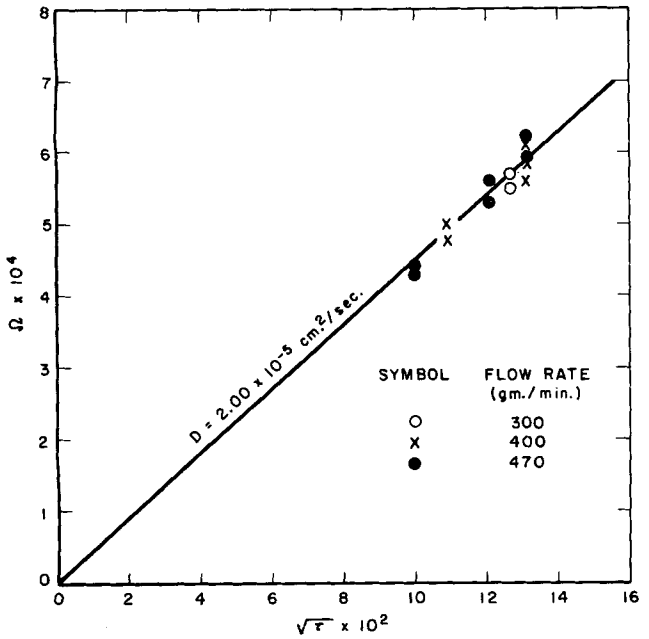

Fig. 2. Argon absorption data at 25°C.

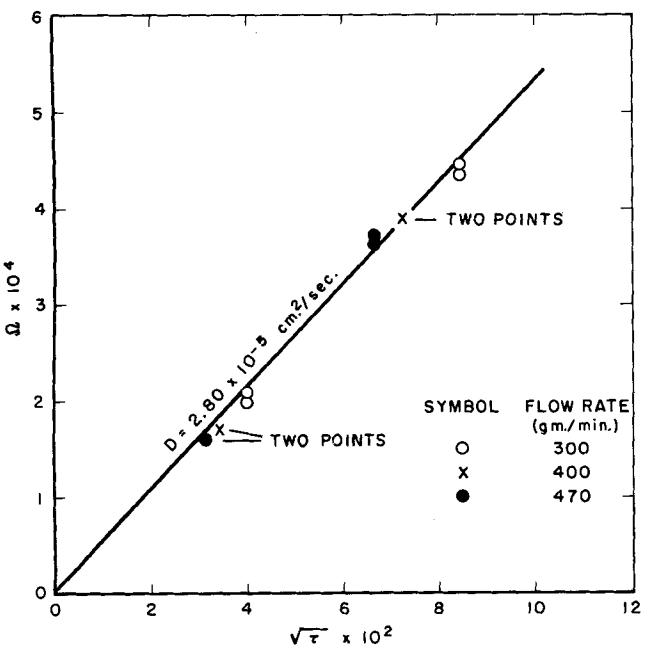

Fig. 3. Carbon dioxide absorption data at 40°C.

value of a dissolved gas in a liquid for calibration purposes and are subject to the uncertainty involved in choosing an accurate calibration value. Among those studies rejected as not being absolute are the investigations of Houghton and co-workers which involve the rate of solution of small gas bubbles. These studies were rejected, since Wise and Houghton (*43*) in the most recent study of this type consider it necessary to use the diffusion of oxygen as a means of determining a cell calibration constant. The subsequent discussion concerning the diffusion of oxygen will show that their choice of a diffusion coefficient for the oxygen-water system is highly questionable. Also rejected in this comparison were the studies of oxygen diffusion by Hagenbach (*14*) and Tammann and Jessen (*36*). The obviously high diffusivity values of these investigations indicate complications introduced by materials which were added to inhibit natural convection.

There have been a diverse number of methods devised for determining diffusion coefficients in the gas-liquid systems studied here. Several of these methods can be classified as unsteady state methods involving quiescent liquid systems (*4, 14, 17, 35*). Forming another general classification are the steady state methods involving laminar flow systems such as laminar jets (*6, 7, 37* to *39*), annular jets (*2*), and wetted spheres (*2, 9*). In addition, there are two studies in which a diaphragm cell technique was employed (*30, 40*), and, finally, there are the polarographic technique (*3, 18* to *21, 34*) and the photochemical method (*22, 26*) which are specific for the study of oxygen diffusion.

Whenever possible, the diffusivity results of all of the methods which involve the use of a gas solubility were corrected to a common solubility value. The use of a standard solubility is essential for a valid comparison, since many of the reported diffusion coefficients are proportional to the reciprocal of the square of the solubility, and there are significant differences in the solubility values that were used in the original references. References to the solubilities used in this comparison are indicated in Table 2.

In Table 3 the results of this study for the carbon dioxide-water system at 25°C. are compared with several previously determined values. The diffusivity data for this system are so numerous that no attempt was made to include all of the existing data in this comparison. Table 3 shows a representative sample of all the existing data at 25°C. Except for the low value of Unver and Himmelblau (*39*), the laminar jet data are in good agreement and appear to be as accurate as any technique that is now available.

Table 3. Comparison of Carbon Dioxide Diffusivities in Water at 25°C.

$D \times 10^5$, sq. cm./sec.	Investigator	Method	Reference number
1.98	This study	Laminar jet	
1.88	Clarke	Laminar jet	7
1.87	Davidson and Cullen	Wetted sphere	9
1.87	Scriven	Diaphragm cell	30
1.87	Tang and Himmelblau	Laminar jet	37
1.96	Thomas and Adams	Laminar jet	38
1.65	Unver and Himmelblau	Laminar jet	39
2.00	Vivian and King	Diaphragm cell	40

All diffusivities have been corrected to a carbon dioxide solubility of 3.303×10^{-6} g. mole/cc.

Comparison with Previous Data

In order to establish the accuracy of the laminar jet experiment and the developed method of analysis, all previous measurements of diffusivities for the six systems studied were collected for comparison. Methods which are not absolute were not included in the comparison (*11* to *13, 16, 27, 43*). These are defined as methods which depend on the use of at least one predetermined diffusivity

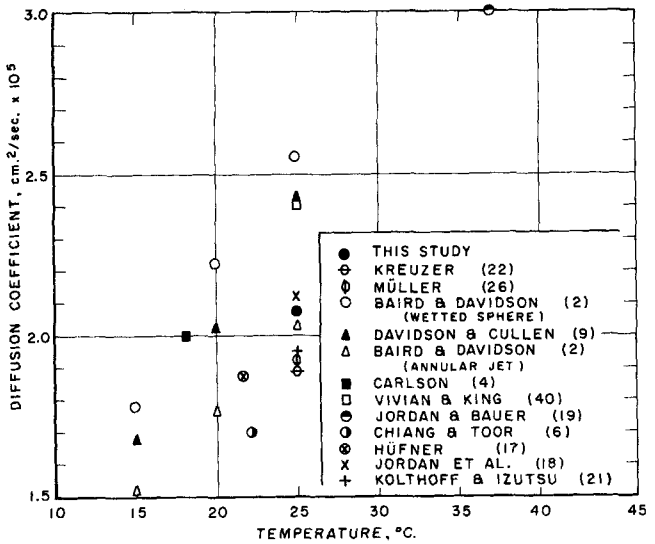

Fig. 4. Experimental diffusion coefficients for oxygen-water system.

The collection of diffusivity data for the oxygen-water system obtained by a variety of methods is shown as a function of temperature in Figure 4. The polarographic technique involving the measurement of the limiting current caused by the diffusion of oxygen to a polarized dropping mercury electrode is particularly useful for the study of oxygen diffusion. The relationship between the measured current and the diffusion coefficient can be obtained from a perturbation solution to the problem of diffusion to an expanding spherical sink (*24*). The classical solution to this problem which includes only one perturbation term is commonly referred to as the *Ilkovic equation* and has been used by most investigators in the analysis of their data. However, recently it has been shown that to obtain accurate diffusivity data a modified Ilkovic equation including the second perturbation term must be employed (*21*). The incorporation of the second perturbation term will lower the resulting calculated diffusion coefficient by 10 to 30% under usual conditions, and, consequently, the results of those studies which employed the unmodified Ilkovic equation were not included in this compilation (*3, 20, 34*). Furthermore, the work of Ratcliff and Holdcroft (*29*) indirectly indicates that the polarographic results obtained from the modified Ilkovic equation may be low by from 1 to 3% owing to the presence of electrolytes in the aqueous medium. In addition, the results of the photochemical studies may also be slightly low owing to the presence of hemoglobin as an indicator. In the photochemical technique of Müller (*26*), a 0.03 wt. % hemoglobin solution was used, whereas the studies of Kreuzer (*22*) were performed in a 1% by weight hemoglobin solution.

Figure 4 shows that there are large variations in the existing diffusivity data for the oxygen-water system. The data in this figure can be roughly categorized as belonging to two distinct groups. There are several data points in one group which indicate a higher diffusivity behavior with a value of approximatey 2.5×10^{-5} sq.cm./sec. at 25°C. and numerous data points which fall into a lower grouping indicating a diffusion coefficient at 25°C. of approximately 2.0×10^{-5} sq.cm./sec. The commonly accepted values for the oxygen-water system have been the data in the higher range (*6, 15*). However, we believe close examination of the experimental evidence tends to support a lower diffusivity behavior. The experimental data in the upper group are the results of four studies (*2, 4, 9, 40*), two of which involve the use of a wetted sphere apparatus. Although no complete analysis was developed for the complex flow situation around the sphere, Davidson and co-workers were able to obtain values for the diffusivity of carbon dioxide which are consistent with existing data. It is interesting to note, however, that for almost all of the other systems studied by these investigators, the diffusion coefficients obtained are consistently higher than the existing data. Furthermore, the carbon dioxide diffusivity data of Carlson (*4*) are also significantly higher than other data available for this system in this temperature range as compiled by Himmelblau (*15*). The elimination of natural convection currents in a quiescent system such as that used by Carlson is quite difficult, and small currents can cause a significant increase in the apparent diffusion coefficient. Hence, some doubt is cast on Carlson's value for oxygen diffusivity.

It is evident from Figure 4 that the results of eight independent studies involving five different experimental techniques give evidence in support of an oxygen diffusivity lower than that commonly accepted. The acceptance of a lower diffusivity value for oxygen will have some significant implications. For example, Wise and Houghton (*43*) use an oxygen diffusivity of 2.6×10^{-5} sq.cm./sec. at 25°C. to calculate a cell constant in their dissolving bubble experiments. However, their diffusivity results for all the gases studied are consistently high in comparison with other available data, and a significant improvement would be realized if a lower oxygen diffusivity were used in the calibration.

The diffusivity behavior of the other gases studied are presented in Figures 5 through 8. In these figures solid lines connecting common data points of each specific investigation have been drawn as visual aids. Only very limited data are available for these systems, and it is not possible to reach many general conclusions. However, it is readily evident from the data in Table 3 as well as Figures 7 and 8 that the results of Unver and Himmelblau (*39*) have a tendency to be low. The results of the present study consistently fall between the data of other investigators.

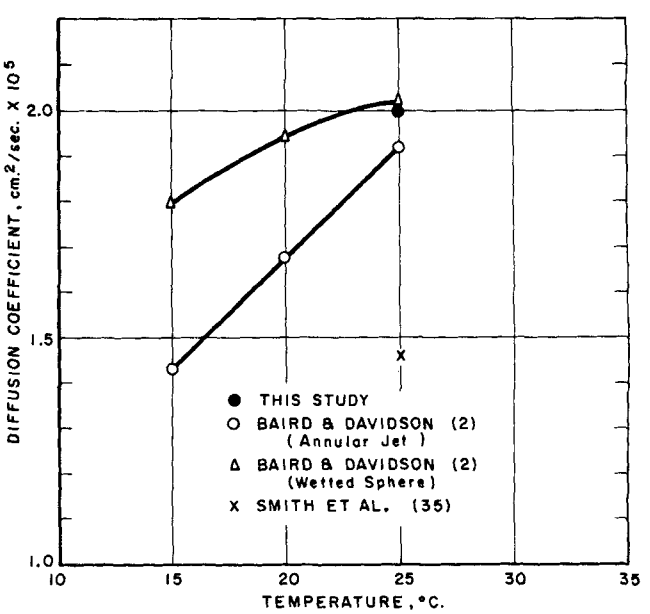

Fig. 5. Experimental diffusion coefficients for argon-water system.

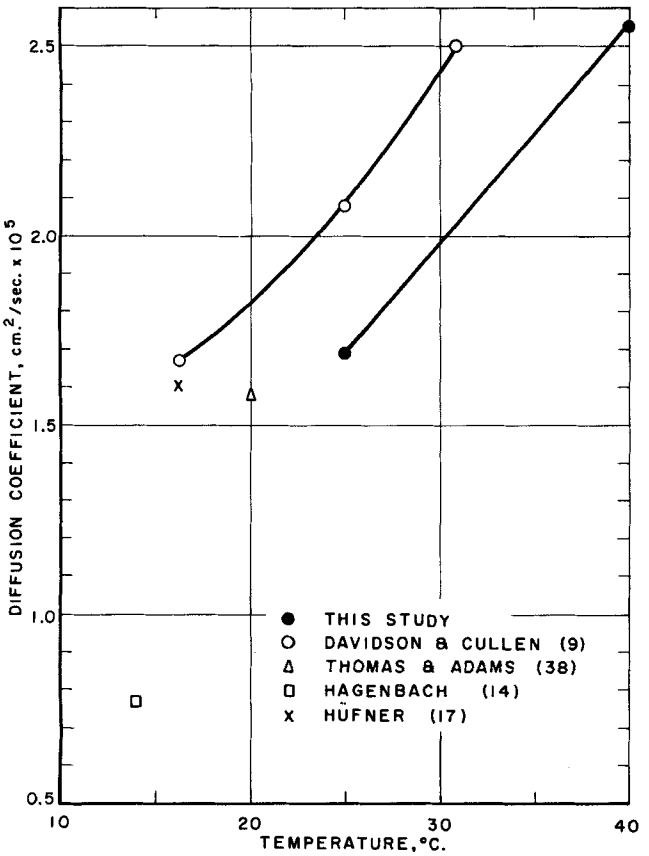

Fig. 6. Experimental diffusion coefficients for nitrous oxide-water system.

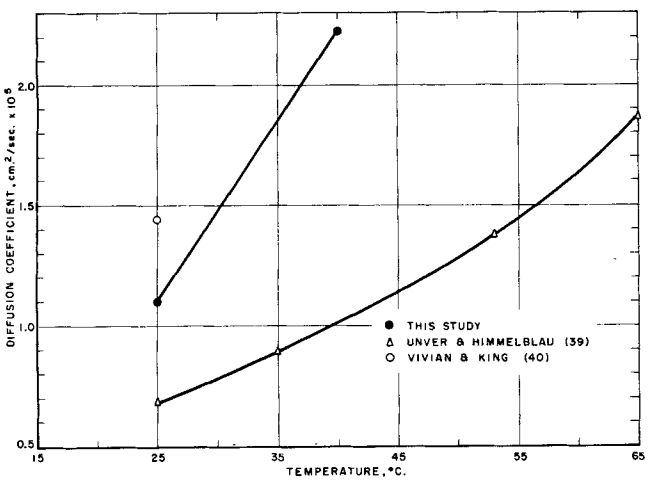

Fig. 7. Experimental diffusion coefficients for ethylene-water system.

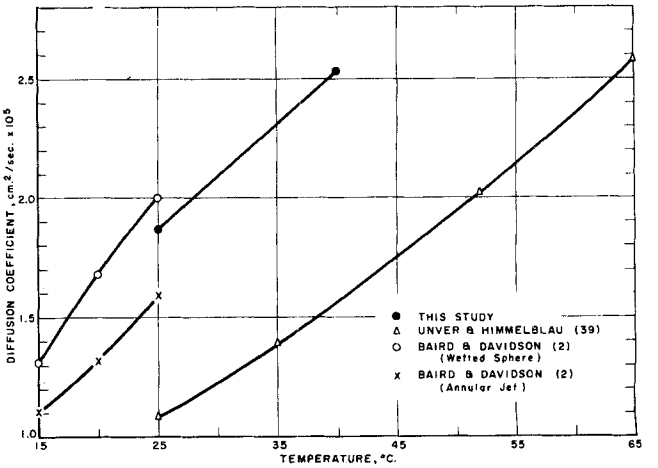

Fig. 8. Experimental diffusion coefficients for propylene-water system.

CONCLUSIONS

The comparison of the diffusivity results of this study with other available data indicates that the developed method of analysis can be used to obtain accurate diffusivity data from laminar jet experiments. This method of analysis eliminates the need for specially designed nozzles which inhibit velocity profile development, and it can readily be adapted to the analysis of absorption data obtained from a jet with a fully developed velocity profile issuing from a straight cylindrical conduit. Such an apparatus would eliminate the very small error introduced by assuming a uniform profile at the entrance of the cylindrical throat of a nozzle. On the other hand, if it is desirable to experimentally minimize the effects of the jet hydrodynamics, this analysis can be used to check the success of such experimental modifications.

Chiang and Toor (*6*) and Baird and Davidson (*2*) have presented data which indicate that a significant interfacial resistance is present in laminar jet diffusion experiments. The arguments of Chiang and Toor are based on the fact that their oxygen diffusivity data obtained with a laminar jet are significantly lower than the value of 2.20×10^{-5} sq.cm./sec. at 22.2°C. which they consider the lowest probable value. The result of an analysis of their experimental data which does not include interfacial resistance effects is shown in Figure 4. It is evident that their value for oxygen diffusivity is in reasonable agreement with the lower group of data points in this figure. Baird and Davidson base their arguments for the existence of a significant interfacial resistance on the fact that the results of their long exposure time experments with wetted spheres are consistently higher than the results of their annular jet experiments. However, it is apparent from the available data that the wetted sphere apparatus has a tendency to give high diffusivity values. Thus, there appears to be no conclusive evidence that demonstrates the existence of a significant interfacial resistance in laminar jet diffusion studies.

Calculations based on the kinetic theory predict that interfacial resistance effects, although always present, should be completely negligible even at the short contact times characteristic of jets, and there should exist essentially phase equilibrium at the gas-liquid boundary except for an extremely short distance in the vicinity of the nozzle. In the absence of surface-active agents, therefore, one could only conclude that the interfacial resistance is of negligible importance in the typical laminar jet experiment unless, of course, there is experimental evidence to the contrary. The evidence cited by Chiang and Toor and by Baird and Davidson is suspect for the reasons noted above. The greater part of the data for both carbon dioxide and oxygen, which have probably been studied as extensively as any gases, shows the jet results to be in substantial agreement with other methods. Hence, the preponderance of the evidence favors introducing a phase equilibrium assumption into the jet analysis. There has been, in our opinion, no conclusive evidence to the contrary, and

utilizing this assumption is more plausible than postulating an interfacial resistance at an uncontaminated gas-liquid interface. It must, therefore, be concluded from the present evidence that the laminar jet experiment represents a rapid and accurate method of obtaining diffusion coefficients of dissolved gases in liquids.

ACKNOWLEDGMENT

The authors wish to acknowledge the work of W. L. Sigelko who constructed the equipment and collected all of the experimental data. D. J. Sundquist and R. W. Rolke also assisted in the early stages of the investigation.

NOTATION

D = binary diffusion coefficient
g = acceleration of gravity
$\bar{g}$ = determinant of space metric tensor in Protean coordinate system
g^{ij} = associated space metric tensor
$g(\psi)$ = function defined by Equation (7)
j_I^i = i^{th} component of mass diffusion flux of component I relative to mass average velocity
N_{Fr} = Froude number = $U_a^2/2R_0g$
N_I = mass of gas absorbed per unit time per unit area
N_J = dimensionless group defined by Equation (3)
N_{Re} = Reynolds number = $2R_0\rho U_a/\mu$
N_{Sc} = Schmidt number = $\mu/\rho D$
N_{We} = Weber number = $2R_0U_a^2\rho/\sigma$
n^i or n_i = contravariant or covariant component of unit normal vector to phase interface
Q = mass of gas absorbed per unit time
R_s = radius of jet/nozzle radius
R_o = nozzle radius
r = radial distance or radial distance/nozzle radius
U = axial velocity in cylindrical coordinates/U_a
U_a = average axial velocity at nozzle
U_c = dimensionless axial center-line velocity of jet
U_s = dimensionless axial surface velocity of jet
V = radial velocity in cylindrical coordinates/U_a
V_s = dimensionless radial surface velocity of jet
v^i = i^{th} component of mass average velocity
X^i = space coordinate variable
Y = independent variable defined by Equation (25)

Greek Letters

ζ = dimensionless coordinate variable = ξ/N_{Re}
η = independent variable defined by Equation (29)
θ = azimuthal coordinate variable
μ = viscosity of liquid
ξ = Protean coordinate variable or Protean coordinate variable/R_o
ρ = total mass density of liquid phase
ρ_I = mass density of component I or dimensionless mass density of component I,

$$\frac{\rho_I - \rho_{IO}}{\rho_{IE} - \rho_{IO}}$$

ρ_I^i = i^{th} order perturbation term for mass density
ρ_{IE} = equilibrium concentration of dissolved gas at interface
ρ_{IO} = inlet concentration of dissolved gas
σ = surface tension
τ = independent variable defined by Equation (42)
ϕ = variable defined by Equation (2)
ψ = Protean coordinate variable or Protean coordinate variable/$R_o^2U_a$
Ω = variable defined by Equation (53)
ω_I = mass fraction of component I
Bar refers to Protean coordinates

LITERATURE CITED

1. Azarnoosh, A., and J. J. McKetta, *J. Chem. Eng. Data*, **4**, 211 (1959).
2. Baird, M. H. I., and J. F. Davidson, *Chem. Eng. Sci.*, **17**, 473 (1962).
3. Brdicka, R., and K. Wiesner, *Coll. Czech. Chem. Commun.*, **12**, 39 (1947).
4. Carlson, T., *J. Am. Chem. Soc.*, **33**, 1027 (1911).
5. Carslaw, H. S., and J. C. Jaeger, "Conduction of Heat in Solids," Oxford Univ. Press, Oxford, England (1959).
6. Chiang, S. H., and H. L. Toor, *AIChE J.*, **5**, 165 (1959).
7. Clarke, J. K. A., *Ind. Eng. Chem. Fundamentals*, **3**, 239 (1964).
8. Cullen, E. J., and J. F. Davidson, *Trans. Faraday Soc.*, **53**, 113 (1957).
9. Davidson, J. F., and E. J. Cullen, *Trans. Inst. Chem. Engrs.*, **35**, 51 (1957).
10. Duda, J. L., and J. S. Vrentas, *Chem. Eng. Sci.*, **22**, 855 (1967).
11. Exner, F., *Pogg. Ann.*, **155**, 321 (1875).
12. *Ibid.*, 443.
13. Gertz, K. H., and H. H. Loeschcke, *Z. Naturforsch.*, **9b**, 1 (1954).
14. Hagenbach, A., *Wied. Ann.*, **65**, 673 (1898).
15. Himmelblau, D. M., *Chem. Rev.*, **64**, 527 (1964).
16. Houghton, G., P. D. Ritchie, and J. A. Thomson, *Chem. Eng. Sci.*, **17**, 221 (1962).
17. Hüfner, G., *Wied. Ann.*, **60**, 134 (1897).
18. Jordan, J., E. Ackerman, and R. L. Berger, *J. Am. Chem. Soc.*, **78**, 2979 (1956).
19. Jordan, J., and W. E. Bauer, *ibid.*, **81**, 3915 (1959).
20. Kolthoff, I. M., and C. S. Miller, *ibid.*, **63**, 1013 (1941).
21. Kolthoff, I. M., and K. Izutsu, *ibid.*, **86**, 1275 (1964).
22. Kreuzer, F., *Helv. Physiol. Acta.*, **8**, 505 (1950).
23. Kunerth, W., *Phys. Rev.*, **19**, 512 (1922).
24. Levich, V. G., "Physicochemical Hydrodynamics," Prentice-Hall, Englewood Cliffs, N. J. (1962).
25. Linke, W. F., "Solubilities of Inorganic and Metal Organic Compounds," 4 ed., Vol. 1, Van Nostrand, New York (1958).
26. Müller, A., *Helv. Physiol. Acta.*, **6**, 21 (1948).
27. Pircher, L., *ibid.*, **10**, 110 (1952).
28. Raimondi, Pietro, and H. L. Toor, *AIChE J.*, **5**, 86 (1959).
29. Ratcliff, G. A., and J. G. Holdcroft, *Trans. Inst. Chem. Engrs.*, **41**, 315 (1963).
30. Scriven, L. E., Ph.D. thesis, Univ. Delaware, Newark (1956).
31. Scriven, L. E., and R. L. Pigford, *AIChE J.*, **5**, 397 (1959).
32. Seidell, A., "Solubilities of Inorganic and Metal Organic Compounds," 3 ed., Vol. 1, Van Nostrand, New York (1940).
33. *Ibid.*, Vol. 2 (1941).
34. Semerano, G., L. Riccoboni, and A. Foffani, *Gazz. chim. ital.*, **79**, 395 (1949).
35. Smith, R. E., E. T. Friess, and M. F. Morales, *J. Phys. Chem.*, **59**, 382 (1956).
36. Tammann, G., and V. Jessen, *Z. Anorg. Allg. Chem.*, **179**, 125 (1929).
37. Tang, Y. P., and D. M. Himmelblau, *Chem. Eng. Sci.*, **20**, 7 (1965).
38. Thomas, W. J., and M. J. Adams, *Trans. Faraday Soc.*, **61**, 668 (1965).
39. Unver, A. A., and D. M. Himmelblau, *J. Chem. Eng. Data*, **9**, 428 (1964).
40. Vivian, J. E., and C. J. King, *AIChE J.*, **10**, 220 (1964).
41. Vrentas, J. S., J. L. Duda, and K. G. Bargeron, *ibid.*, **12**, 837 (1966).
42. Vrentas, J. S., Ph.D. thesis, Univ. Delaware, Newark (1963).
43. Wise, D. L., and G. Houghton, *Chem. Eng. Sci.*, **21**, 999 (1966).

Manuscript received March 28, 1967; revision received July 13, 1967; paper accepted July 17, 1967.